Applied Catalysis B: Environmental 160–161 (2014) 135–143

Contents lists available at ScienceDirect

Applied Catalysis B: Environmental

journal homepage: www.elsevier.com/locate/apcatb

Hydrothermal stability of Pd/ZrO_2 catalysts for high temperature methane combustion

Jung-Hyun Park[a], Jun Hee Cho[a], Yun Jung Kim[a], Eun Seok Kim[b], Hyun Sik Han[b], Chae-Ho Shin[a,*]

[a] Department of Chemical Engineering, Chungbuk National University, Chungbuk 361-763, Republic of Korea
[b] R&D Center, Heesung Catalysts Corp., #507-1Da, Jungwang-Dong, Shiheung-City, Kyungki-Do 429-450, Republic of Korea

ARTICLE INFO

Article history:
Received 11 October 2013
Received in revised form 8 May 2014
Accepted 9 May 2014
Available online 16 May 2014

Keywords:
Methane combustion
Palladium
Zirconia
Calcination effect
Hydrothermal stability

ABSTRACT

A monoclinic ZrO_2 support was synthesized via a precipitation technique for the investigation of the effects of calcination temperature on methane combustion over Pd/ZrO_2 and $Pd/\gamma\text{-}Al_2O_3$ catalysts at 600 °C, in the absence and presence of water vapor. In comparison with $Pd/\gamma\text{-}Al_2O_3$, all the Pd/ZrO_2 catalysts studied showed superior performances. With the exception of Pd/ZrO_2 (ZrO_2 support calcined at 1000 °C), all the Pd/ZrO_2 catalysts showed higher methane conversions in the presence of water vapor than in its absence. The Pd/ZrO_2 catalyst with a ZrO_2 support calcined at 900 °C exhibited the highest activity as well as the greatest durability under both conditions, in spite of its low surface area. Transmission electron microscopy indicated that the activity of methane combustion is unrelated to Pd particle size. In addition, the results of temperature-programmed decomposition of Pd oxide on Pd/support and X-ray photoelectron spectroscopy showed that the activity of Pd/ZrO_2 was strongly dependent on the oxidation state of the Pd species.

© 2014 Elsevier B.V. All rights reserved.

1. Introduction

Methane is present in emissions from a variety of natural gas processes, such as from electrical utilities, coke ovens, farms, and vehicles [1–4]. Partly because of the influence of methane on the greenhouse effect, methane emissions have become of great environmental concern [5]. Therefore, it is important to totally oxidize methane and remove as much of the unburned hydrocarbon as possible prior to its release into the atmosphere.

The conventional thermal combustion of methane requires very high temperatures (up to 1600 °C), resulting in production of noxious by-products such as NO_x. Catalytic combustion has been proposed as a method for promoting the effective oxidation of hydrocarbons, while simultaneously lowering emissions of NO_x, CO, VOCs, and unburned hydrocarbons. In addition, this method is a good route for purifying gases released from various industrial facilities, such as natural gas-fueled engines and boilers [6–8]. High catalytic activities and hydrothermal stabilities are required for superior catalytic species to catalyze methane combustion. However, it is difficult for a catalyst to possess both of these requirements.

In general, Pd-based catalysts are the most active catalyst for the combustion of methane [9,10]. There is extensive literature regarding the relationship between the activity of supported Pd catalysts and the chemical state of Pd, as well as interactions of the support with the active species and Pd dispersion [11–13]. In particular, it is known that the oxidation state of Pd is very important for catalytic methane combustion. For example, Diannan et al. [14] suggested that the active Pd/Al_2O_3 catalyst phase is PdO or mixed Pd^0/PdO. The formation of PdO is dependent on the reaction temperature and oxygen pressure. At above 230 °C and in oxygen exposure conditions, PdO can be formed on supported Pd nanoparticles. This oxide is also formed at the interface between the particles and the support, and then this phase becomes oxidized with increasing an oxidation temperature. The formed PdO crystallites can be decomposed due to the thermodynamic equilibrium in Pd/PdO phase and finally formed as the mixture of metallic Pd and PdO. Thus, both metallic Pd and PdO can be coexisted on the surface and this mixed phase likely work synergistically, supposing that CH_4 activation may be easier on Pd metal, Pd oxide providing O_2 species to form CO_2 for methane combustion [15–17].

* Corresponding author. Tel.: +82 43 261 2376; fax: +82 43 269 2370.
E-mail address: chshin@chungbuk.ac.kr (C.-H. Shin).

http://dx.doi.org/10.1016/j.apcatb.2014.05.013
0926-3373/© 2014 Elsevier B.V. All rights reserved.

Additionally, it was reported that the poor catalytic activity may be due to the presence of inactive PdO_2. Ciuparu and Pfefferle [18] showed that the degree of reduction of Pd on Pd/CeO_2–ZrO_2 catalysts is related to the catalytic activity in methane combustion.

Water vapor is one of the most significant factors affecting the catalytic performances of the aforementioned species. The effect of water on catalytic performance for methane combustion has been investigated by numerous researchers [19–25]. In general, water vapor produced or fed into the reactant has a negative effect on catalytic activity due to the formation of inactive $Pd(OH)_2$ [19,20]. Supported Pd catalysts are usually deactivated by water vapor, regardless of the various supports available, such as Al_2O_3, TiO_2, and SnO_2 [21–23]. Zirconia-supported Pd catalysts show stable activity during reaction in the presence of water vapor [24,25]. However, there are no clear explanations for the deactivation of such catalysts during reaction in the presence of water vapor.

It is well known that the high catalytic activities and hydrothermal stabilities of ZrO_2-suppored Pd catalysts depend on factors, such as the precursor, metal loading, support, calcination temperature, catalyst pretreatment and reaction conditions [26–28]. In this study, ZrO_2 support was synthesized using a chemical precipitation method; investigations of the effects of the calcination temperature were then conducted, with emphasis on examination of methane combustion performance over Pd/ZrO_2 and Pd/γ-Al_2O_3 catalysts at 600 °C, in the absence and presence of water vapor. In particular, this study was concerned specially with the hydrothermal stabilities of the catalysts. Furthermore, the reasons for catalyst deactivation were discussed on the basis of X-ray photoelectron spectroscopy (XPS) results. The reasons for the deficiencies in catalytic hydrothermal stability in practical applications, as well as the main influencing factors for Pd-based catalyst activities, remain unclear.

2. Experimental

2.1. Preparation of catalysts

The ZrO_2 support was synthesized using a chemical precipitation technique through a reflux method at 78 °C. For synthesis of the ZrO_2 support, 14.3 g $ZrOCl_2{\cdot}8H_2O$ (Junsei, ≥90%) was dissolved in a mixture solution consisting of 140 ml deionized water and 60 ml ethanol (the water–ethanol volume ratio is 2.3:1). 4 M NH_4OH (Samchun, ≥28%, 120 ml) was added slowly until the solution pH reached a value of 10, and was then heated to 78 °C and maintained at that temperature for 1 h with vigorous stirring. The resulting white precipitate was filtered and washed with deionized water to remove chloride ions. The obtained precipitate was dried in an oven at 100 °C for 24 h. In order to examine the effects of the support calcination temperature on catalytic performance, the dried samples were calcined in the range of 700–1000 °C for 6 h in air.

Catalysts of composition 0.5 wt% Pd/ZrO_2 were prepared by the incipient wetness impregnation method using a $Pd(NH_3)_4Cl_2$ (Aldrich, ≥99.99% metals basis) solution on a ZrO_2 support pretreated at different calcination temperatures and calcined at 800 °C for 10 h in air. Prior to synthesis of the Pd/ZrO_2 catalyst, 0.5 wt% Pd stock solution was prepared by dissolving the 0.6189 g $Pd(NH_3)_4Cl_2$ in a 50 ml deionized water. The 3 ml stock solution was used for the impregnation on 3 g ZrO_2 support. To compare the performance of Pd/ZrO_2 in methane combustion, Pd/γ-Al_2O_3 (γ-Al_2O_3: Procatalyse, 194 $m^2\,g^{-1}$, particle size between 100 and 150 μm) catalyst was synthesized as a reference sample through the above described impregnation route. A number in parentheses after Pd/ZrO_2, e.g., (700) refer to the calcination temperature of the ZrO_2 support and this style is used throughout.

2.2. Catalyst characterization

The specific surface areas and pore volumes were determined by N_2 physisorption at −196 °C using a Micromeritics ASAP2020 apparatus. The catalysts (0.5 g) were first degassed for 6 h at 250 °C. Specific surface area was calculated in the relative pressure range 0.01–0.2, assuming a cross-sectional area of 0.162 nm^2 for the N_2 molecule. To identify the crystalline phases of Pd, ZrO_2 and Al_2O_3, X-ray diffraction (XRD) patterns were obtained with a Bruker D5000 diffractometer using Cu-Kα radiation at 50 mA and 30 kV. In addition, the size and dispersion of the supported particles were measured by transmission electron microscopy (TEM) (Tecnai G2 F30), operated at 300 kV. The chemical states of the Pd species on the catalyst surface were identified by XPS on an ESCALAB 210 Electron Spectrometer (Al Kα radiation; $h\nu$ = 1486.6 eV). The XPS data were calibrated using the binding energy of C1s (284.6 eV) as the standard.

The temperature-programmed decomposition (TPD) experiments with Pd oxide on Pd/ZrO_2 and Pd/γ-Al_2O_3 (O_2-TPD) were carried out on a Micromeritics AutoChem II 2920 instrument using a thermal conductivity detector. The catalyst (0.2 g) was fixed in a quartz reactor by packing quartz wool at both ends. Prior to the measurement, the sample was oxidized in a 5% O_2 in He flow (50 $cm^3\,min^{-1}$) at 800 °C for 0.5 h. After cooling the sample under a 5% O_2 in He flow to room temperature, the feed gas was switched to a He stream (50 $cm^3\,min^{-1}$) for O_2-TPD. The sample was heated at a rate of 10 °C min^{-1} from room temperature to 800 °C.

Temperature-programmed reduction of methane (CH_4-TPR) experiments was carried out using the same reaction apparatus. The catalyst (0.1 g) was loaded in a U-shaped quartz reactor and the analysis was performed without any pretreatment. The reactant was CH_4 (1 vol.%)-N_2 with a total flow rate of 50 $cm^3\,min^{-1}$ was continuously passed through the reactor while the sample was heated at a rate of 10 °C min^{-1} from 100 to 600 °C. The consumption of methane in reaction effluent gas was analyzed online using a methane analyzer (Teledyne Analytical Instrument 7500 IR gas analyzer).

2.3. Activity test

Isothermal and temperature programmed methane combustion (TPMC) were conducted using a fixed-bed reactor under atmospheric pressure. Prior to the activity tests, the catalysts (particle size between 100 and 150 μm) were pretreated at 800 °C for 0.5 h under flowing purified N_2 (200 $cm^3\,min^{-1}$). After cooling to 600 °C, an isothermal catalytic activity and stability tests were examined on the reaction mixture consisting 1 vol.% CH_4, 20 vol.% O_2 and 79 vol.% N_2 with a total flow rate of 200 $cm^3\,min^{-1}$ (120,000 $cm^3\,g_{cat}{}^{-1}\,h^{-1}$). In addition, the effect of water vapor was examined by adding a continuous flow of 3% water vapor by bubbling of water in saturator, which could be controlled by the variation of saturator temperature. Also, TPMC was performed with a heating rate 4 °C min^{-1} from 200 and to 800 °C in the presence or absence of water vapor. The concentration of methane was analyzed online every 2 s using a methane analyzer (Teledyne Analytical Instrument 7500 IR gas analyzer). Although the data were collected every 2 s, they were shown with an interval of 20 °C for the exact comparison of catalytic performance among the catalysts examined.

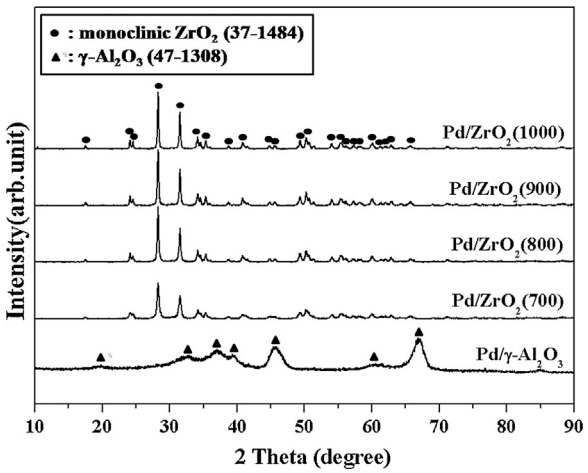

Fig. 1. XRD patterns of Pd/γ-Al_2O_3 and Pd/ZrO_2 catalysts calcined at 800 °C for 6 h. The ZrO_2 support was pre-calcined at different temperatures before impregnation of Pd.

3. Results and discussion

3.1. XRD analysis

The XRD patterns of the calcined Pd/ZrO_2 and Pd/γ-Al_2O_3 catalysts are shown in Fig. 1. The XRD analysis of Pd/ZrO_2 showed only a monoclinic phase. The crystallinity of ZrO_2 was found to increase with increasing calcination temperature. For all the catalysts used in this study, no obvious PdO or Pd peaks were observed, due to the low Pd loading and the overlapping of the ZrO_2 peaks [29].

3.2. Physical properties

The specific surface areas and total pore volumes of the calcined Pd/ZrO_2 and Pd/γ-Al_2O_3 catalysts are summarized in Table 1. The specific surface area of the Pd/ZrO_2 catalyst decreased with increasing calcination temperature of the support; specially, specific surface area was reduced greatly from 16.4 to 0.7 $m^2\,g^{-1}$ as the calcination temperature increased from 700 to 1000 °C. The pore volume of the Pd/ZrO_2 catalyst also decreased with increasing calcination temperature of the support. Sintering of ZrO_2 particles is thought to be the cause of this phenomenon. The specific surface area and pore volume of Pd/γ-Al_2O_3 were much larger than those of the ZrO_2 supported catalysts, determined as 143 $m^2\,g^{-1}$ and 0.433 $cm^3\,g^{-1}$, respectively. Although a large specific surface area in ZrO_2 is important for fostering catalytic activity in relation to high dispersion of the active metal, the monoclinic ZrO_2 support commonly possesses quite small values. The specific surface area of Pd/ZrO_2 (900) appeared to be smaller than those of the other catalysts examined, except for Pd/ZrO_2 (1000); however, this sample showed the best activity (see Figs. 3 and 4). In addition, the Pd/ZrO_2 (900) after 100 h reaction showed very low specific surface area with 1 $m^2\,g^{-1}$.

Table 1
Physical properties of Pd/ZrO_2 and Pd/γ-Al_2O_3 catalysts.

Catalyst[a]	S_{BET} ($m^2\,g^{-1}$)	Total pore volume ($cm^3\,g^{-1}$)
Pd/ZrO_2 (700)	16.4	0.059
Pd/ZrO_2 (800)	7.4	0.037
Pd/ZrO_2 (900)	1.1	0.005
Pd/ZrO_2 (1000)	0.7	0.003
Pd/γ-Al_2O_3	143	0.433

[a] The number in parentheses is the calcination temperature of ZrO_2 support.

3.3. TEM analysis

The size and morphology of Pd particles integrated into the catalysts were examined with TEM. The TEM images of the Pd/ZrO_2 and Pd/γ-Al_2O_3 catalysts are shown in Fig. 2. Spherical small Pd particles with 3–5 nm size were observed on the Pd/ZrO_2 (700) surfaces. In particular, large agglomerated and bulky Pd clusters with above 20 nm were found for the Pd/ZrO_2 (800), Pd/ZrO_2 (900) and Pd/ZrO_2 (1000) catalysts. For the Pd/ZrO_2 (900) and Pd/ZrO_2 (1000) catalysts, quasi-core shell shaped clusters were observed, which indicated strong interactions between the support and the Pd particles [27,30] On the Pd/γ-Al_2O_3 catalyst, the spherical Pd particles with 7–10 nm size were found on surfaces. This phenomenon is clearly different from those of ZrO_2 supported catalysts.

3.4. Catalytic combustion of methane

The catalytic performance of the supported Pd catalysts was investigated as a function of reaction temperature for temperature-programmed methane combustion in the absence or presence of water vapor (Fig. 3 and Table 2). The catalytic performance is strongly dependent on the support calcination temperature. For the comparison of $T_{light\text{-}off}$, the catalytic activity in dry conditions decreased in the following order; Pd/γ-Al_2O_3 > Pd/ZrO_2 (900) > Pd/ZrO_2 (1000) > Pd/ZrO_2 (800) > Pd/ZrO_2 (700). At moderate temperature below 450 °C, Pd/ZrO_2 (800–1000) catalysts were more active than Pd/γ-Al_2O_3 catalyst. Under wet reaction conditions, Pd/ZrO_2 (900) catalyst was the most active among catalysts tested. In addition, the catalytic performances of supported Pd catalysts in methane combustion are shown as a function of time on stream at 600 °C in Fig. 4 and Table 2. The activities and stabilities of the Pd/ZrO_2 catalysts for methane combustion strongly varied with the calcination temperature of the support employed. The Pd/γ-Al_2O_3, Pd/ZrO_2 (700), and Pd/ZrO_2 (800) catalysts showed relatively high deactivation phenomena in the absence of water vapor. In particular, the methane conversion over Pd/γ-Al_2O_3 significantly decreased from 95.2% to 79.7% with 15 h on stream. The thermal stability of the catalyst is thought to be one of the main factors impacting catalytic performance, with deactivation of Pd/γ-Al_2O_3 mainly caused by the transformation of PdO to Pd at temperatures above 500 °C [27,30]. The Pd/ZrO_2 catalytic system exhibited higher hydrothermal stabilities than the Pd/γ-Al_2O_3 catalyst. In methane combustion, water is generally considered to be an inhibitor of catalyst activation [19,32,33]. However, with the exception of Pd/ZrO_2 (1000), all the Pd/ZrO_2 catalysts examined indicated the reverse tendency. In this study, water vapor is generally thought to be helpful for oxidation of the Pd metal state. The maximum catalytic activity among the Pd/ZrO_2 series examined was achieved using Pd/ZrO_2 (900), under both reaction conditions (presence and absence of water vapor), with activity remaining almost constant during the 15 h reaction. The Pd/ZrO_2 catalyst was thus found to exhibit a higher stability than the Pd/γ-Al_2O_3 species in the presence of water vapor. Although the details are not yet known, this observed higher stability in the presence of water vapor would probably result from the relatively high hydrophobicity of ZrO_2 inhibiting phase transitions in the Pd particles, such as the formation of inactive $Pd(OH)_2$ species [23,24]. However, Pd/ZrO_2 (1000) showed the poorest hydrothermal stability. This may be explained by the fact that relatively larger amounts of bulk Pd particles exist on the surface of ZrO_2 calcined at 1000 °C. These species, having weak interactions with the support, might undergo accelerated transformation to $Pd(OH)_2$ in the presence of water vapor. From a practical point of view, Pd/ZrO_2 (900) can be considered to be the most effective among the catalysts examined.

To assess the stability of the catalyst, a long-term test of the Pd/ZrO_2 (900) and Pd/γ-Al_2O_3 catalysts was carried out in the

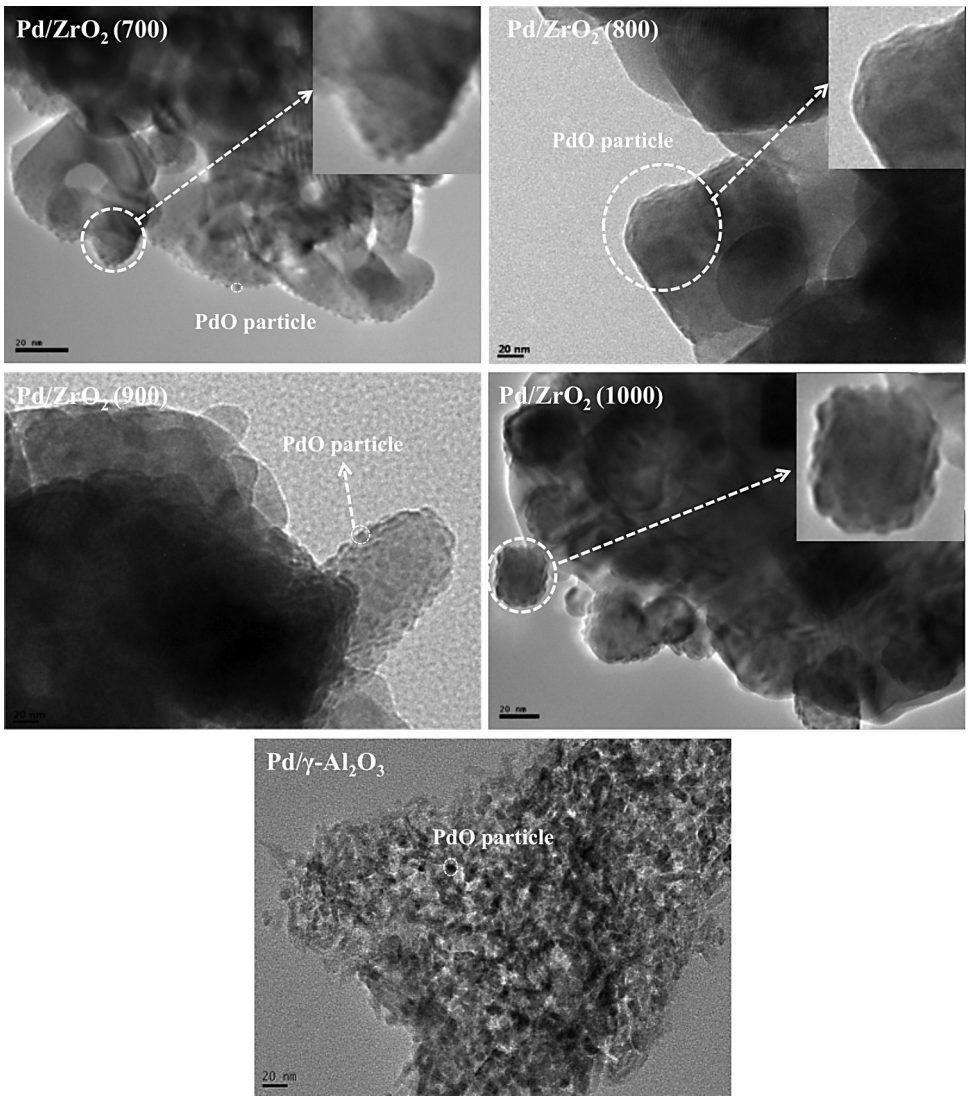

Fig. 2. TEM images of Pd/γ-Al_2O_3 and Pd/ZrO_2 catalysts calcined at 800 °C for 6 h. The ZrO_2 support was pre-calcined at different temperatures before impregnation of Pd.

Table 2
Activities for methane combustion of Pd supported catalysts in the absence and presence of 3% water vapor.

Catalysts	TMPC (°C)[a]				Isothermal at 600 °C			
	Dry[b]			Wet[c]			CH_4 conv. (%)[e]	
	$T_{10\%}$	$T_{50\%}$	$T_{90\%}$[d]	$T_{10\%}$	$T_{50\%}$	$T_{90\%}$	Dry	Wet
Pd/ZrO_2 (700)	424	596	–	407	467	633	67.7	53.9
Pd/ZrO_2 (800)	337	427	640	392	436	549	71.0	65.4
Pd/ZrO_2 (900)	344	429	623	366	389	417	93.5	92.9
Pd/ZrO_2 (1000)	384	550	–	370	396	549	91.0	89.3
Pd/γ-Al_2O_3	388	475	563	390	418	449	97.2	82.7

[a] Temperature programmed methane combustion with a heating rate 4 °C min^{-1} from 200 to 800 °C.
[b] 1% CH_4, 20% O_2, and N_2 as balance gas, GHSV = 120,000 h^{-1}.
[c] Continuous addition of 3% water vapor.
[d] Temperature reached to 10, 50, and 90% methane conversion, respectively.
[e] Obtained after a 15 h methane combustion.

presence of water vapor and the results are shown in Fig. S1. The Pd/ZrO_2 (900) catalyst showed the good catalytic performance and methane conversion after 100 h reaction was found to be ca. 92%. On the other hand, the methane conversion of Pd/γ-Al_2O_3 catalyst was gradually decreased from 97% down to 66% after 100 h reaction. Although the conversion of Pd/ZrO_2 (900) is slightly decreased during the reaction, the Pd/ZrO_2 (900) catalyst showed stable catalytic performance for methane combustion compared to that of Pd/γ-Al_2O_3 catalyst.

3.5. O_2-TPD

To evaluate the relation between catalytic activity and the decomposition properties of PdO on catalysts, O_2-TPD experiments

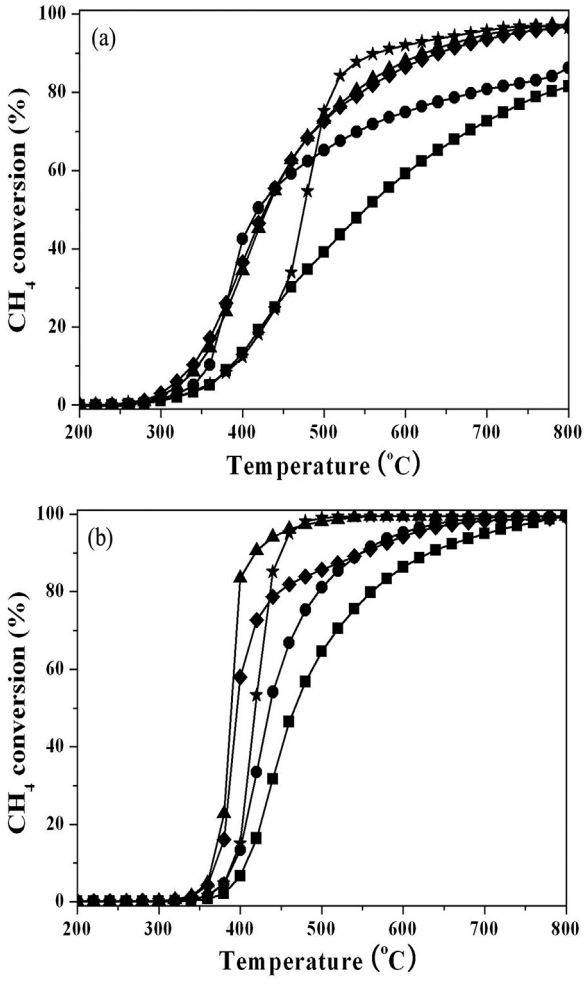

Fig. 3. Catalytic performance for methane combustion as a function of reaction temperature in the (a) absence and (b) presence of water vapor (3%); Pd/ZrO_2 (700) (■), Pd/ZrO_2 (800) (●), Pd/ZrO_2 (900) (▲), Pd/ZrO_2 (1000) (♦) and $Pd/\gamma\text{-}Al_2O_3$ (⋆). Dry conditions: 1% CH_4, 20% O_2, and N_2 as balance gas, GHSV = 120,000 h^{-1}, and wet conditions: continuous addition of 3% water vapor.

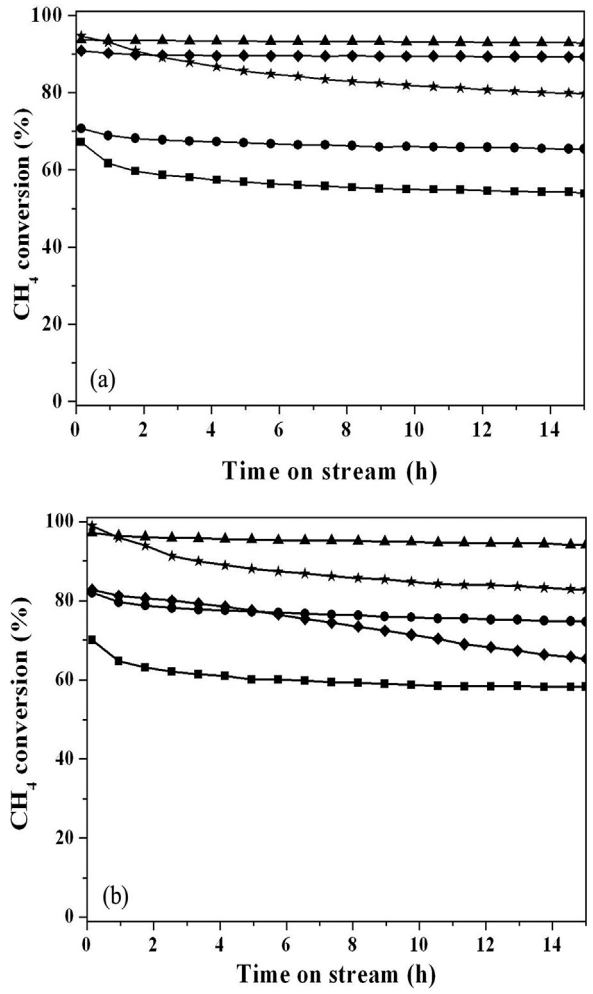

Fig. 4. Effect of calcination temperature of ZrO_2 on catalytic performance for methane combustion as a function of time on stream in the (a) absence and (b) presence of water vapor (3%); Pd/ZrO_2 (700) (■), Pd/ZrO_2 (800) (●), Pd/ZrO_2 (900) (▲), Pd/ZrO_2 (1000) (♦) and $Pd/\gamma\text{-}Al_2O_3$ (⋆). Dry conditions: 1% CH_4, 20% O_2, and N_2 as balance gas, GHSV = 120,000 h^{-1}, and wet conditions: continuous addition of 3% water vapor.

were carried out on $Pd/\gamma\text{-}Al_2O_3$ and Pd/ZrO_2 (Fig. 5). TPD peaks were observed at ca. 530–600 °C and 620–770 °C. These peaks have been attributed to the release of oxygen as PdO decomposes to metallic Pd [8,12,27,31]. The PdO on ZrO_2 supported catalysts calcined below 800 °C was not decomposed below 600 °C. However, decomposition of the remaining catalysts resulted in two different types of species. The first peak at low temperatures (530–600 °C) for $Pd/\gamma\text{-}Al_2O_3$, Pd/ZrO_2 (900), and Pd/ZrO_2 (1000) can be attributed to the decomposition of a thermodynamically unstable bulk PdO species, as suggested by Yang et al. [8]. The second peak, which is observed at ca. 620 °C, can be attributed to the decomposition of a stabilized PdO species, as suggested by Sekizawa et al. [27]. Therefore, it may be inferred that the peak, appearing in the higher temperature region is attributable to the decomposition of PdO under a strong support interaction [12,27,31]. Peaks observed at 670–720 °C shifted to a higher temperature with increasing ZrO_2 support calcination temperature with the exception of the support calcined at 1000 °C. The decomposition temperature of Pd (620–770 °C) decreased in the following order: Pd/ZrO_2 (900) > Pd/ZrO_2 (1000) > Pd/ZrO_2 (800) > Pd/ZrO_2 (700). Un-symmetric peaks in the O_2-TPD profile of $Pd/\gamma\text{-}Al_2O_3$ were observed at ca. 500–750 °C. The position of the peak was shifted to a lower temperature, compared with the decomposition temperature of PdO on the Pd/ZrO_2 catalysts. This increase in

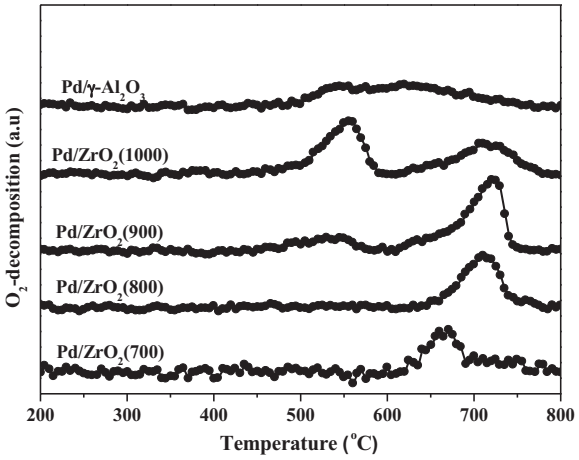

Fig. 5. Evolution of TCD signals during O_2-TPD of PdO in $Pd/\gamma\text{-}Al_2O_3$ and Pd/ZrO_2 catalysts. The ZrO_2 support was pre-calcined at different temperatures before impregnation of Pd.

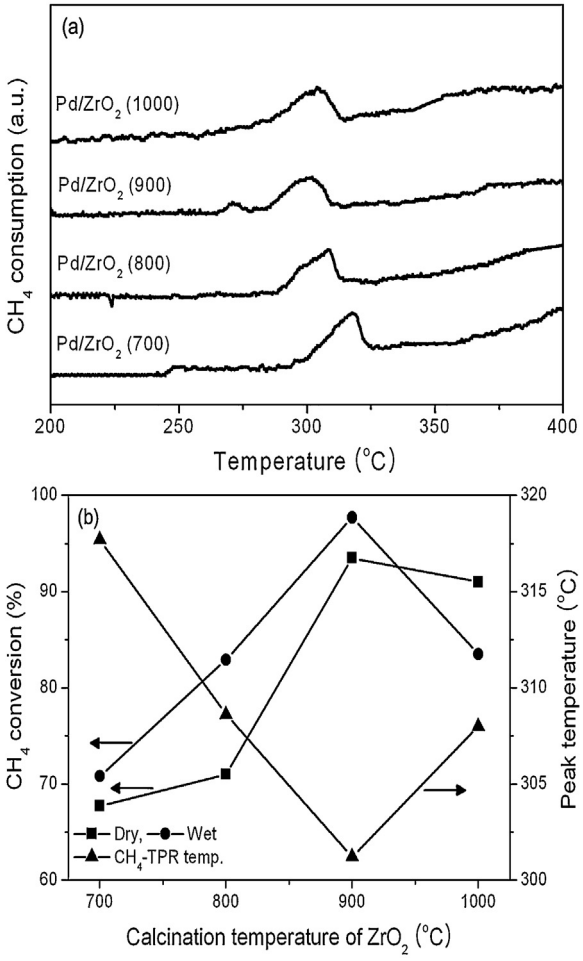

Fig. 6. (a) CH_4-TPR profiles of Pd/ZrO_2 catalyst with different calcination temperatures of ZrO_2, and (b) the correlation curve between initial catalytic activities and reduction temperature of the catalysts in CH_4-TPR.

decomposition temperature is indicative of a stronger interaction between Pd species and the support [12,27,31].

The decomposition temperature of PdO, observed as a second peak above 600 °C, can be correlated to the catalytic activity in methane combustion. The best catalytic activity under the experimental operating conditions was shown over Pd/ZrO_2 (900), which has the highest PdO decomposition temperature (715 °C) and relatively abundant peak intensity. Therefore, it can be considered that the interaction between the active metal species and the support are very important in determining catalytic activity.

3.6. CH_4-TPR

To evaluate the reduction behavior of PdO, CH_4-TPR experiments were carried out on Pd/ZrO_2 catalysts (Fig. 6). The TPR profiles were observed to contain two major peaks. The high-temperature peak (>400 °C, not shown) can be attributed to the reforming of methane over reduced Pd particles [34]. Therefore, only at lower temperature (<400 °C) can the reduction properties of the PdO species be observed. CH_4 consumption and CO_2 release during the TPR analysis are in agreement with the stoichiometry of PdO reduction by CH_4 [33] ($4PdO + CH_4 \rightarrow 4Pd + CO_2 + H_2O$). The low-temperature peaks could be divided into various peaks corresponding to different PdO species reacting with CH_4. The crystalline phase of PdO is known to be reduced more readily than amorphous Pd [36]. Thus, peaks ascribed to the crystalline PdO species and amorphous PdO species could be differentiated

Table 3
XPS data for Pd/ZrO_2 (900) catalysts obtained at different reaction stages.

Reaction stage	Binding energy (eV)			Atomic ratio	
	Zr $3p_{3/2}$	Pd $3d_{5/2}$		Pd^{2+}/Pd^0	Pd/Zr
		Pd^0	Pd^{2+}		
Fresh[a]	332.5	335.3	336.6	8.1	0.177
Pretreatment[b]	332.3	335.3	336.8	0.7	0.066
After reaction (a)[c]	332.4	335.3	336.6	7.3	0.156
After reaction (p)[d]	332.4	335.3	336.6	7.9	0.161

[a] Catalyst calcined at 800 °C for 10 h in air.
[b] Catalyst pretreated at 800 °C for 0.5 h in N_2.
[c] Catalyst after 15 h on stream in the absence of water vapor.
[d] Catalyst after 15 h on stream in the presence of water vapor.

by their observed reduction temperatures. The reduction peaks were observed to shift to a lower temperature with increasing ZrO_2 calcination temperature. Of the examined materials, Pd/ZrO_2 (900) exhibited the lowest temperature and reduction tendency, with the observed order of reactivity being as follows: Pd/ZrO_2 (900) > Pd/ZrO_2 (1000) > Pd/ZrO_2 (800) > Pd/ZrO_2 (700).

As shown in Fig. 6(b), the maximum activity was shown over Pd/ZrO_2 (900) catalyst under both reaction conditions. In contrast, the minimum reduction temperature was shown over this catalyst according to CH_4-TPR analysis. Combined with the initial conversion for CH_4 combustion, the catalytic activity could be correlated with the reduction temperature tendency of the catalysts (Fig. 6(b)). Similar observations have been described in previous literature reports [35,37].

3.7. XPS analysis

The surface Pd species of Pd/ZrO_2 (900) catalysts at varying reaction stages were characterized by XPS, and the results are shown in Fig. 7 and Table 3. Because the peaks of Pd $3d_{5/2}$ and Zr $3p_{3/2}$ overlapped in the spectrum of Pd/ZrO_2, these peaks were deconvoluted into three Gaussian peaks [38]. The binding energies of $Pd3d_{5/2}$ were 335.3 and 336.7 ± 0.1 eV, which can be assigned to Pd and PdO, respectively [14,38]. As can be seen in Fig. 6 and Table 3, various Pd oxide species were created on the catalyst surface after calcination. However, after pretreatment under an N_2 flow, most of the PdO had decomposed to Pd, which indicates that thermal decomposition of PdO occurs at 700–800 °C. This is in agreement with the O_2-TPD results. Before and after pretreatment, the Pd^{2+}/Pd^0 atomic ratios of the catalyst surface were 8.1 and 0.7, respectively. These values had changed to 7.3 and 7.9 after the reaction in the absence of water vapor and in its presence, respectively. It is apparent that, after the reaction in the presence of water vapor, the Pd^{2+}/Pd^0 atomic ratio increased, compared with the reaction in the absence of water vapor, this result is possibly associated with the increase in methane combustion activity upon exposure to water vapor.

It can be considered that catalytic activity is correlated to the Pd^{2+}/Pd^0 atomic ratios of the Pd/ZrO_2 catalysts. This may result from the fact that metallic Pd is oxidized with relative ease in the presence of water vapor, as the initial reaction progresses at the pre-reduced metallic Pd state. These results suggest that the oxidation state of the Pd is vital in the combustion reaction of methane. Pre-reduction of the catalyst is shown to be effective for the formation and/or maintenance of the active phase during the reaction, and therefore, enhances the activity of the catalyst [39].

Table 3 also presents the surface Pd/Zr atomic ratios values of Pd $3d_{5/2}$ and Zr $3p_{3/2}$ at different reaction stages. The atomic ratios of Pd/Zr are initially high and decrease after pretreatment, recovering partially after reaction in both the absence and presence of water

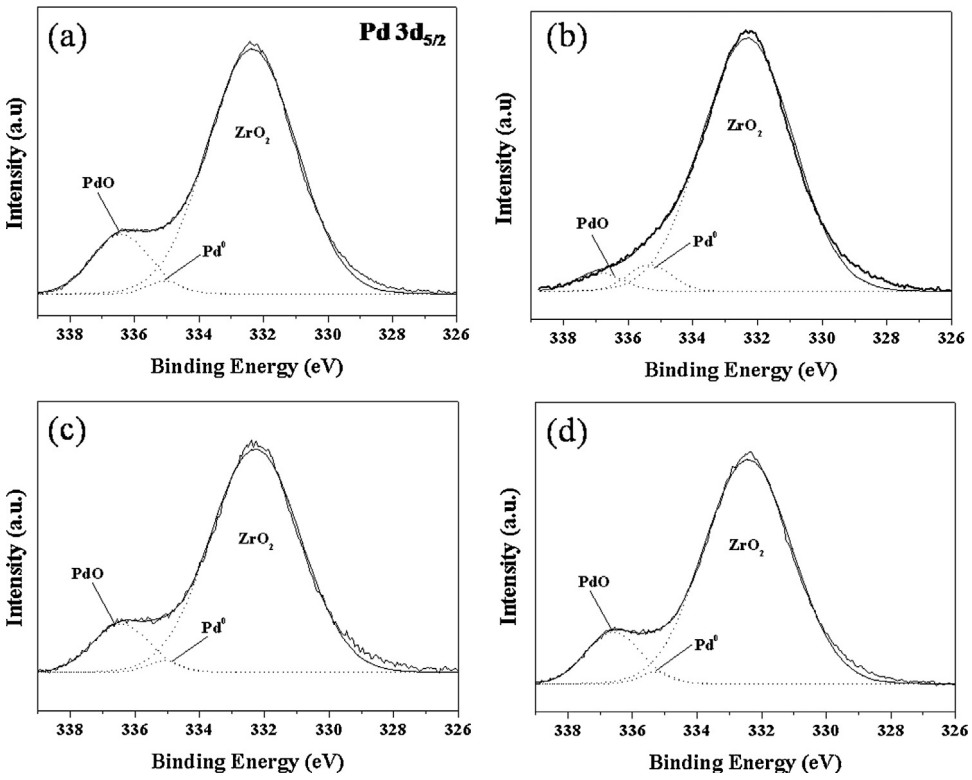

Fig. 7. XP spectra of Pd/ZrO_2 (900) catalyst at different reaction stages: (a) catalyst calcined at 800 °C for 10 h in air; (b) catalyst pretreated at 800 °C for 0.5 h in N_2; (c) catalyst after reaction in the absence of water vapor; and (d) catalyst after reaction in the presence of water vapor (3%).

vapor. This result can be explained by the decomposition of PdO and its agglomeration into large metallic Pd particles. In addition, the results can be further explained by the recycling mechanism between Pd and PdO proposed by Farrauto et al. [40]. The Pd/Zr atomic ratio after reaction in the absence of water vapor was observed to be lower than in the presence of water vapor. It is speculated that this outcome may be attributed to the existence of large metallic Pd particles formed by partial oxidation of large metallic Pd after pretreatment. In order to examine the relationship between the chemical state of the Pd atoms in the catalyst and its catalytic activity, surface composition and atomic ratio values were calculated from the XP spectra, and are shown in Fig. 8. According to the results, in the presence of water vapor, the activities of the Pd/ZrO_2 catalysts were higher than in its absence (Figs. 3 and 4). These trends were obtained for all the ZrO_2-supported Pd catalysts studied, except for Pd/ZrO_2 (1000). According to Fig. 8(a), after methane combustion in the absence of water vapor, the Pd^{2+}/Pd^0 atomic ratios of Pd/ZrO_2 calcined at 700, 800, 900 and 1000 °C decreased in the following order: Pd/ZrO_2 (900) > Pd/ZrO_2 (1000) > Pd/ZrO_2 (800) > Pd/ZrO_2 (700). As can be seen in Fig. 8, the catalytic activity tendency was in agreement with the XPS results in the presence of water vapor as well as in its absence. This suggests that Pd catalyst activity is strongly dependent on the oxidation state of Pd, indicating that the PdO phase or Pd/PdO mixture is more active than the metallic state. It is generally agreed that during the reaction, especially under an oxygen-rich atmosphere, PdO is the main active phase [1,14,18,41]. However, in the case of the Pd/ZrO_2 (1000) catalyst, the initial activity in the absence of water vapor was observed to be higher than that in the presence of water vapor, with similarly poor stability observed during the reaction with water vapor present. It can be inferred from these results that further heating of the Pd/ZrO_2 catalyst at 1000 °C lead to significant deactivation, resulting in lower catalytic activities of the methane oxidation in the presence of water vapor. This can be explained by the fact that

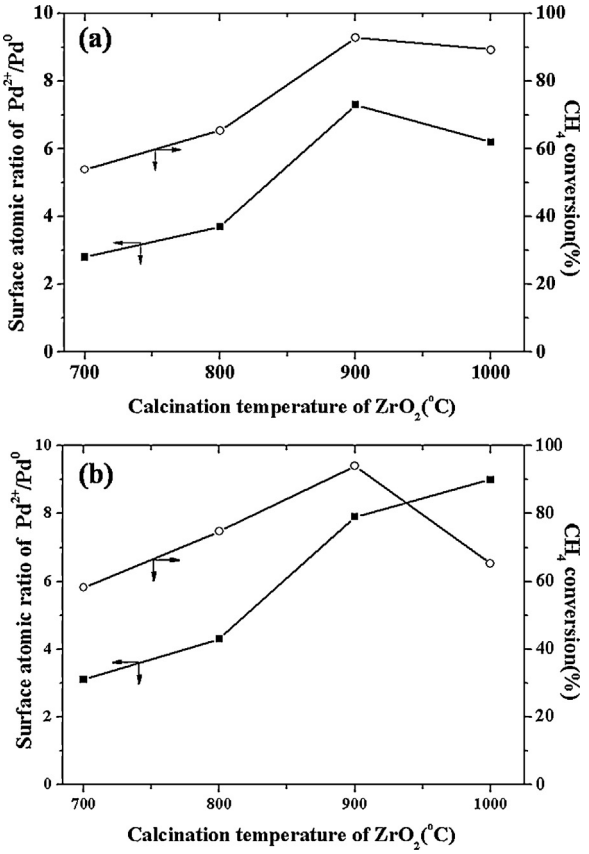

Fig. 8. Pd^{2+}/Pd^0 atomic ratio dependence of catalytic activity for Pd/ZrO_2 catalysts with support calcined at different temperatures after reaction in: (a) the absence, and (b) the presence of water vapor (3%).

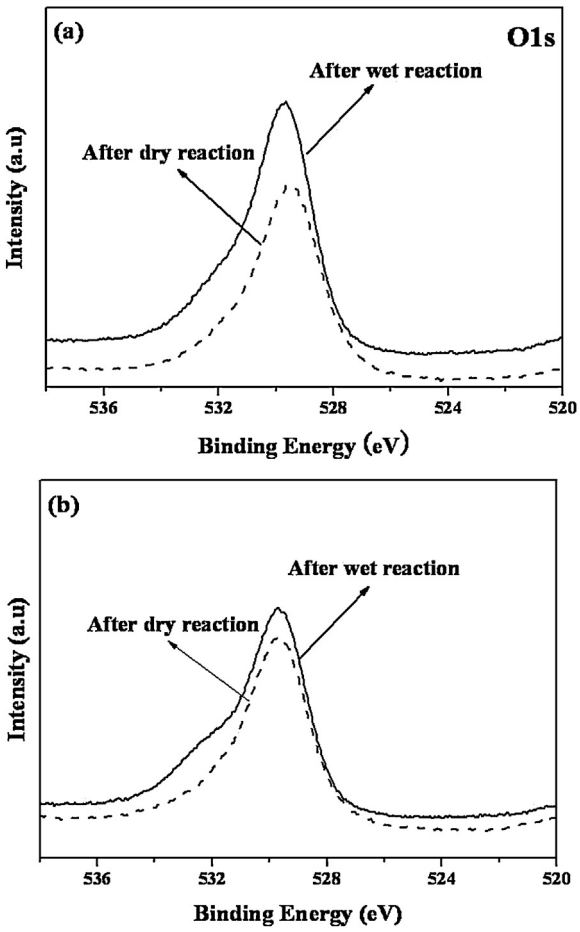

Fig. 9. O1s XP spectra of (a) Pd/ZrO_2 (900) and (b) Pd/ZrO_2 (1000) catalysts after reaction in the absence and presence of water vapor (3%).

relatively large amounts of bulk Pd particles exist on the surface of ZrO_2 calcined at 1000 °C, as shown in the TEM images (see Fig. 2). These species, having a weak interaction with the support, would undergo accelerated transformation to $Pd(OH)_2$ in the presence of water vapor. This explanation agrees well with the O1s XPS results of Pd/ZrO_2 (900), and Pd/ZrO_2 (1000), shown in Fig. 9.

As shown in Fig. 9, the O1s XP spectra exhibited one dissymmetrical peak. This peak could be divided into two different peaks at 529.6 ± 0.1 and 531.9 ± 0.1 eV. According to literatures [21,42], the peaks at 529.6 and 531.9 eV could be assigned to the lattice oxygen in the form of the O^{2-} ion in the oxides and adsorbed non-stoichiometric oxygen species in the form of —OH or as O^- associated with surface defect oxides, respectively. The relative ratio of the O1s peak at 529.6 and 531.9 eV drastically increased after CH_4 combustion reaction in the presence of water vapor. This can be explained by the presence of a large amount of $Pd(OH)_2$, as suggested in the aforementioned studies.

4. Conclusions

The XRD patterns of ZrO_2 supports calcined at different temperatures from 700 to 1000 °C for 6 h showed only the monoclinic phase. In comparison with $Pd/\gamma\text{-}Al_2O_3$, all the Pd/ZrO_2 catalysts showed superior performance toward methane combustion at 600 °C in the absence and presence of water vapor. The catalytic activity of Pd/ZrO_2 changed dramatically depending on the calcination temperature of the ZrO_2 support. In particular, Pd/ZrO_2 (900) displayed the highest activity as well as the greatest durability in the absence and presence of water vapor, in spite of its low BET surface area. From the results of O_2-TPD, CH_4-TPR and XPS, it was shown that the activity of Pd/ZrO_2 was strongly dependent on the oxidation state of the Pd species. The stable PdO species above 600 °C mainly contributed to the enhanced stabilized catalytic activity in high temperature methane combustion. These results demonstrate that the nature of the support is an important factor in the control of catalytic activity in methane combustion.

Acknowledgement

This work was financially supported by a grant from the Industrial Source Technology Development Programs (2013-10033479) of the Ministry of Trade, Industry and Energy (MOTIE) of Korea.

Appendix A. Supplementary data

Supplementary data associated with this article can be found, in the online version, at http://dx.doi.org/10.1016/j.apcatb.2014.05.013.

References

[1] P. Gélin, M. Primet, Appl. Catal. B: Environ. 39 (2002) 1–37.
[2] C. Amairia, S. Fessi, A. Ghorbel, J. Sol-Gel Sci. Technol. 54 (2010) 29–35.
[3] L.S. Escandon, S. Ordonez, A. Vega, F.V. Dıez, J. Hazard. Mater. 153 (2008) 742–750.
[4] J. Li, X. Liang, S. Xu, J. Hao, Appl. Catal. B: Environ. 90 (2009) 307–312.
[5] http://epa.gov/climatechange/ghgemissions/gases/ch4.html
[6] A. Baylet, S. Royer, P. Marecot, J.M. Tatibouet, D. Duprez, Appl. Catal. B: Environ. 77 (2008) 237–247.
[7] L.F. Liotta, G. Di Carlo, G. Pantaleo, G. Deganello, Catal. Commun. 6 (2005) 329–336.
[8] L. Yang, C. Shi, X. He, J. Cai, Appl. Catal. B: Environ. 38 (2002) 117–125.
[9] D. Ciuparu, E. Perkins, L. Pfefferle, Appl. Catal. A: Gen. 263 (2004) 145–153.
[10] R.J. Farrauto, M.C. Hobson, T. Kennelly, E.M. Waterman, Appl. Catal. A: Gen. 81 (1992) 227–237.
[11] K. Sekizawa, K. Eguchi, H. Widjaja, M. Machida, H. Arai, Catal. Today 28 (1996) 245–250.
[12] H. Yoshida, T. Nakajima, Y. Yazawa, T. Hattori, Appl. Catal. B: Environ. 71 (2007) 70–79.
[13] J.M. Sohn, S.K. Kang, S.I. Woo, J. Mol. Catal. A 186 (2002) 135–144.
[14] D. Gao, C. Zhang, S. Wang, Z. Yuan, S. Wang, Catal. Commun. 9 (2008) 2583–2587.
[15] S. Specchia, E. Finocchio, G. Busca, P. Palmisano, V. Specchia, J. Catal. 263 (2009) 134–145.
[16] C. Binet, M. Daturi, J.-C. Lavalley, Catal. Today 50 (1999) 207–225.
[17] T. Schalow, B. Brandt, M. Laurin, S. Schauermann, S. Guimond, H. Kuhlenbeck, J. Libuda, H.-J. Freund, Surf. Sci. 600 (2006) 2528–2542.
[18] D. Ciuparu, L. Pfefferle, Appl. Catal. A: Gen. 218 (2001) 197–209.
[19] R. Butch, F.J. Urbano, P.K. Loader, Appl. Catal. A: Gen. 123 (1995) 173–184.
[20] G. Diannan, W. Sheng, Z. Chunxi, Y. Zhongshan, W. Shudong, Chin. J. Catal. 29 (2008) 1221–1225.
[21] W. Li, Y. Lin, Y. Zhang, Catal. Today 83 (2003) 239–245.
[22] D. Ciuparu, L. Pfefferle, Appl. Catal. A: Gen. 209 (2001) 415–428.
[23] P. Araya, S. Guerrero, J. Robertson, F.J. Gracia, Appl. Catal. A: Gen. 283 (2005) 225–233.
[24] K. Nomura, K. Noro, Y. Nakamura, H. Yoshida, A. Satsuma, T. Hattori, Catal. Lett. 58 (1999) 127–130.
[25] C. Amairia, S. Fessi, A. Ghorbel, J. Sol-Gel. Sci. Technol. 52 (2009) 260–266.
[26] K. Muto, N. Katada, M. Niwa, Appl. Catal. A: Gen. 134 (1996) 203–215.
[27] K. Sekizawa, H. Widjaja, S. Maeda, Y. Ozawa, K. Eguchi, Appl. Catal. A: Gen. 200 (2000) 211–217.
[28] K. Sekizawa, H. Widjaja, S. Maeda, Y. Ozawa, K. Eguchi, Catal. Today 59 (2000) 69–74.
[29] K. Persson, A. Ersson, S. Colussi, A. Trovarelli, S.G. Jaras, Appl. Catal. B: Environ. 66 (2006) 175–185.
[30] K. Eguchi, H. Arai, Appl. Catal. A: Gen. 222 (2001) 359–367.
[31] Y. Ozawa, Y. Tochihara, A. Watanabe, M. Nagai, S. Omi, Appl. Catal. A: Gen. 258 (2004) 261–267.
[32] J.-H. Park, B. Kim, C.-H. Shin, G. Seo, S.H. Kim, S.B. Hong, Top. Catal. 52 (2009) 27–34.
[33] L.S. Escandon, D. Nino, E. Diaz, S. Ordonez, F.V. Diez, Catal. Commun. 9 (2008) 2291–2296.
[34] U. Oemar, K. Hidajat, S. Kawi, Appl. Catal. A: Gen. 402 (2011) 176–187.

[35] P. Castellazzi, G. Groppi, P. Forzatti, A. Baylet, P. Marécot, D. Duprez, Catal. Today 155 (2010) 18–26.
[36] M.-F. Luo, Z.-Y. Pu, M. He, J. Jin, L.-Y. Jin, J. Mol. Catal. A 260 (2006) 152–156.
[37] C.-K. Shi, L.-F. Yang, Z.-C. Wang, X.-E. He, J.-X. Cai, G. Li, X.-S. Wang, Appl. Catal. A: Gen. 243 (2003) 379–388.
[38] M. Schmal, M.M.V.M. Souza, V.V. Alegre, M.A.P. Silva, D.V. Cesar, C.A.C. Perez, Catal. Today 118 (2006) 392–401.
[39] J.H. Lee, D.L. Trimm, Fuel Process. Technol. 42 (1995) 339–359.
[40] R.J. Farrauto, J.K. Lampert, M.C. Hobson, E.M. Waterman, Appl. Catal. B: Environ. 6 (1995) 263–270.
[41] S. Yang, A.M. Valiente, M.B. Gonzalez, I.R. Ramos, A.G. Ruiz, Appl. Catal. B: Environ. 28 (2000) 223–233.
[42] A. Machocki, T. Ioannides, B. Stasinska, W. Gac, G. Avgouropoulos, D. Delimaris, W. Grzegorczyk, S. Pasieczna, J. Catal. 227 (2004) 282–296.